Available online at www.sciencedirect.com
SCIENCE DIRECT®
Journal of Molecular Catalysis A: Chemical 209 (2004) 125–134
JOURNAL OF MOLECULAR CATALYSIS A: CHEMICAL
www.elsevier.com/locate/molcata

Copper-modified mesoporous MCM-41 silica: FTIR and catalytic study

T. Tsoncheva [a,*], Tz. Venkov [b], M. Dimitrov [a], C. Minchev [a], K. Hadjiivanov [b]

[a] *Institute of Organic Chemistry, Bulgarian Academy of Sciences, 1113 Sofia, Bulgaria*
[b] *Institute of General and Inorganic Chemistry, Bulgarian Academy of Sciences, 1113 Sofia, Bulgaria*

Received 30 April 2003; received in revised form 11 August 2003; accepted 14 August 2003

Abstract

Copper modified MCM-41 silica materials obtained by various preparation techniques are characterized by X-ray diffraction (XRD), temperature programmed reduction (TPR) and FTIR spectroscopy of adsorbed CO. The copper state in the samples is controlled by the preparation method used. The catalytic activity and selectivity of the samples in methanol dehydrogenation are also compared. The role of different copper species in the catalytic process is discussed.

Keywords: Cu/MCM-41; Methanol decomposition; FTIR spectroscopy; Adsorption; CO; Carbonyls

1. Introduction

The products of methanol dehydrogenation are of considerable interest because of their application as an alternative fuel or source for the chemical industry. Among them, methyl formate (MF) is stated as an important intermediate for the production of valuable chemicals such as formic and acetic acids, formaldehyde and dimethylformamide [1–4]. On the other hand, when decomposed to hydrogen and carbon monoxide, methanol is considered to be promising effective and ecological fuel for fuel cells, gas turbines and vehicles [5–9]. Copper-containing materials are usually proposed as suitable low temperature catalysts for these processes [9–33]. MF is often assumed to be an intermediate in methanol decomposition to hydrogen and carbon monoxide, but their direct formation from methanol is not excluded either [17,28,30,34,35]. However, despite the great number of papers dealing with the mechanism of methanol dehydrogenation [11–33,36–48], the problem concerning its selectivity regulation is not fully solved. The selectivity is essentially affected by the acid–basic properties of the support [21–24,27], copper oxidation state and dispersion [19,29,42] and the type of copper precursor used [15,27]. Higher MF selectivity is usually observed with lower methanol conversion, but a significant selectivity decrease with temperature rise and flow rate decrease is also established [9,13,26,30,35,42,46,49].

Recently, mesoporous MCM-41 silicas have provoked a large interest as catalytic supports for metals, metal oxides and organometallic compounds [50–53] due to their well defined porous structure and inertness in catalytic processes. Different methods for the preparation of copper-containing MCM materials have been described [54–56]. Depending on the method used, the presence of copper ions and highly dispersed Cu_2O or CuO particles has been observed.

One of the most widely applied techniques for characterization of copper-containing catalysts is IR spectroscopy of adsorbed CO. It is established that only Cu^+ cations form stable carbonyls [57]. They are usually observed in two spectral regions: (1) around 2160 cm^{-1} (with most zeolite samples [58–63]) and around 2130 cm^{-1} (when copper is supported on oxides [60,64–71]). At high CO equilibrium pressures Cu^+ ions in zeolites form dicarbonyls, and even tricarbonyls at low temperatures [58–63]. Formation of dicarbonyls was also proposed recently for oxide-supported copper [64–66]. The Cu^{2+}–CO bond is mainly electrostatic and, as a result, the Cu^{2+} sites form carbonyls at low temperatures and/or high CO equilibrium pressures only. These species are typically observed around 2200 cm^{-1}. The Cu^0–CO type carbonyls are usually detected below 2100 cm^{-1} [72]. However, in some cases (when the copper dispersion is high or the surface is rough) the Cu^0–CO bands can be found at higher frequencies, in the region

* Corresponding author. Tel.: +3592-979-3961; fax: +3592-8700-225.
E-mail address: ormm@orgchm.bas.bg (T. Tsoncheva).

1381-1169/$ – see front matter © 2003 Elsevier B.V. All rights reserved.
doi:10.1016/j.molcata.2003.08.008

where the Cu^{+}–CO species absorb [73]. In this case a criterion for discrimination between the Cu^{+}–CO and Cu^{0}–CO species is their stability: the carbonyls of metallic copper are easily decomposed during evacuation [57].

In our previous studies, different copper species depending on the preparation method used for copper loaded MCM-41 and MCM-48 materials were established [67,74,75]. A significant amount of copper ions strongly interacting with the support were observed with the samples obtained from the corresponding acetylacetonate [67,74] or ammonia precursor [76]. In the present paper, representative copper modified MCM-41 samples obtained by the above methods were studied in detail by FTIR spectroscopy of adsorbed CO and in catalytic dehydrogenation of methanol. The aim of this study is to clarify the effect of the state of copper originating from the different preparation techniques used on the process selectivity towards methyl formate, carbon monoxide and hydrogen. Some aspects of the reaction mechanism are discussed.

2. Experimental

2.1. Materials

The parent silica MCM-41 material (978 $m^2\,g^{-1}$) were synthesized by a standard procedure described elsewhere [74]. Different copper-containing samples were obtained by the following preparation techniques:

- *Sample CM1*: Two grams of the parent material were stirred at room temperature with 85 ml 0.024 M aqueous solution of $Cu(NO_3)_2$. The liquid phase was removed by a 4 h treatment at 323 K in a rotary evaporator.
- *Sample CM2*: Two grams of the parent material were stirred at room temperature with 11 ml 1 M aqueous solution of $Cu(NO_3)_2$. Then the liquid phase was removed by centrifugation and the obtained product was dried at room temperature and then under vacuum for one night.
- *Sample CM3*: Two grams of the parent material were stirred for 1 h at room temperature and then for one more hour at 323 K with 80 ml 0.023 M solution of copper acetylacetonate in chloroform. The chloroform was then removed in a rotary evaporator.
- *Sample CM4*: Two grams of the parent material were stirred for 1 h in 0.05 M solution of Cu^{2+} then filtered, washed thoroughly with water and dried. The Cu^{2+} solution was prepared by dissolving $Cu(NO_3)_2{\cdot}3H_2O$ in distilled water followed by addition of concentrated NH_3 until a pH value of nine was reached.

After drying all samples were calcined in an air flow at 770 K for 6 h. Samples containing 6–8 wt.% copper (Table 1) and a BET surface area of 700–850 $m^2\,g^{-1}$ were obtained.

2.2. Methods

The IR spectra were recorded on a Nicolet Avatar 360 spectrometer at a spectral resolution of 2 cm^{-1} accumulating 64–128 scans. For the adsorption experiments, self-supporting pellets were prepared from the sample powders and treated directly in the purpose-made IR cell. The latter was connected to a vacuum-adsorption apparatus with a residual pressure below 10^{-4} Pa. The cell allowed the IR measurements to be performed both at ambient temperature and at 100 K. Carbon monoxide (>99.997) was supplied by Merck. Prior to the adsorption measurements, the samples were activated by heating for 1 h in oxygen at 673 K and 1 h evacuation at the same temperature (oxidized samples) within the cell system. To obtain the "reduced" samples, the pellets were treated in hydrogen (27 hPa) for 1 h at 523 or 673 K and then evacuated at 573 K for 1 h.

Powder X-ray diffraction (XRD) data were collected at room temperature with an automatic DRON-3 diffractometer using Cu Kα radiation. Patterns were recorded within the range 30–45° 2θ with a constant step 0.02° 2θ and 1s per step counting time.

The BET surface area and pore diameters were determined by nitrogen adsorption/desorption isotherms at 77 K using a static volumetric technique (Quantachrome Autosorb 1). Before the physisorption measurements the calcined samples were outgassed at 393 K for 15 h under vacuum.

The temperature programmed reduction—thermogravimetric analysis (TPR-TGA) studies were performed in a SETARAM TGDTA 92 microbalance. The samples (usually

Table 1
TPR data on the investigated samples

Sample	Cu (wt.%)	T_{max}* (K)	Weight loss (mg)				Reduction degree** (%)
			Experimental		Theoretical		
			420–500 K	500–870 K	1 h–870 K	Cu^{2+}–Cu^{0}	
CM1	5.60	450	0.52	0.00	0.05	0.57	100
CM2	8.27	450	0.76	0.12	0.08	0.96	100
CM3	5.21	440	0.38	0.03	0.05	0.57	81
CM4	5.94	450	0.14	0.19	0.12	0.61	74

* Temperature of the reduction maximum on the DTG curves.
** Total weight loss during reduction referred to the calculated theoretical weight loss for the reduction of Cu^{2+} to metallic copper.

40 mg) were heated in a flow of 50 vol.% H_2 in Ar (100 $cm^3\,min^{-1}$) up to 873 K at 5 $K\,min^{-1}$ and a final hold-up of 1 h. Prior to the TPR experiments the samples were treated in situ with an air flow up to 873 K at a rate of 10 $K\,min^{-1}$.

The methanol dehydrogenation to MF, CO and H_2 was conducted at 450–700 K in a regime of thermoprogrammed reaction (heating rate 2 $K\,min^{-1}$) or under isothermal conditions at 600 K with Ar as a carrier gas. Practically no other products were detected except for a small amount of CH_4 (about 2–3%) at high temperatures in some cases. The on-line gas chromatographic analysis was made on a Porapak Q and a molecular sieve column using an absolute calibration method. The methanol pressure was 1.57 kPa and WHSV, 1.5 h^{-1}. Before the catalytic experiments the samples were pretreated in situ in air at 773 K for 2 h. To study reduced samples, additional treatment in a flow of a 1:1 mixture of H_2 and Ar at 523 K for 2 h was performed. Product analysis was carried out by on-line gas chromatography. MF selectivity (S_{MF}) was calculated as $X_{MF}/(X_{MF}+X_{CO})$, where X_{MF} and X_{CO} are the MF and CO yields, respectively.

3. Results

3.1. XRD and TPR measurements

Powder X-ray measurements were carried out in order to obtain information about the CuO dispersion depending on the preparation method used (Fig. 1). CM1 and CM2 samples show some typical hkl reflections (at $2\Theta = 35.6$ and 38.8°) of CuO. In contrast, only very weak and broad or no reflections of crystalline CuO were observed for CM3 and CM4 samples, respectively (Fig. 1). These results show different dispersion of the copper oxide in the samples. They also suggest the existence of very small, XRD amorphous CuO particles and/or isolated copper ions with the latter two samples.

The results from the TPR measurements are presented in Fig. 2 and Table 1. A well defined reduction peak with maximum around 450 K is found for all samples in the interval 420–500 K. According to XRD data for analogous samples reduced in hydrogen at 520 K (not shown), this peak could be assigned to reduction of CuO particles to metallic copper. At higher temperatures, 500–870 K, no clearly defined peaks are found. Here, only a tail is observed in the TG profile of the samples. This effect could be assigned to reduction of copper species and/or ions which are more difficult to reduce due to their higher dispersion and stronger interaction with the support. It should be noted that in the case of CM3 and CM4 a considerable fraction of these copper species (19 and 26 wt.%, respectively) could not be reduced even after 1 h at 870 K in a hydrogen flow (Table 1). This indicates the presence of different copper species and suggests that these samples contain also a considerable amount of isolated copper species and ions spread within the host structure.

3.2. FTIR spectra of adsorbed CO

3.2.1. CO adsorption on oxidized CM1

Adsorption of CO (1.3 kPa equilibrium pressure) at 100 K on the vacuum activated sample results in the appearance of two bands with maxima at 2156 and 2136 cm^{-1} (Fig. 3, spectrum a). Both bands strongly decrease in intensity with the equilibrium CO pressure (Fig. 3, spectra b–e) which indicates that they are due to weakly adsorbed species. The band at 2136 cm^{-1} is assigned to physically adsorbed CO and that at 2156 cm^{-1}, to CO H-bonded to surface silanol groups [57]. Indeed, the Si–OH band at 3742 cm^{-1} is shifted to 3635 cm^{-1} in parallel with the appearance/disappearance of the 2156 cm^{-1} band. At lower CO coverages, a weak and broad band centered at 2132 cm^{-1} is clearly visible (Fig. 3,

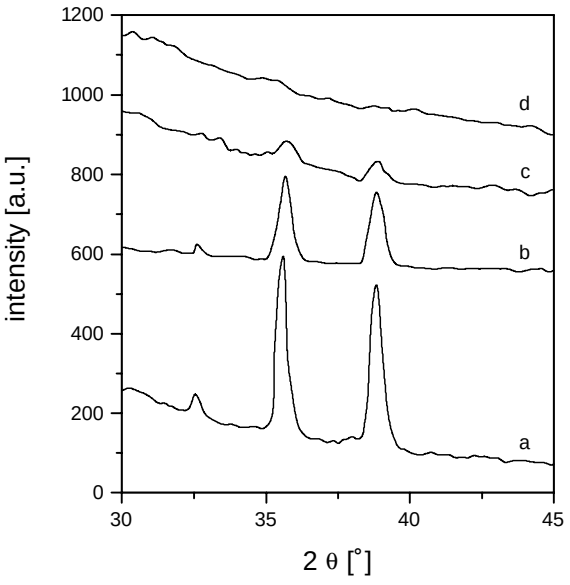

Fig. 1. XRD data on oxidized samples: CM1 (a); CM2 (b); CM3 (c) and CM4 (d).

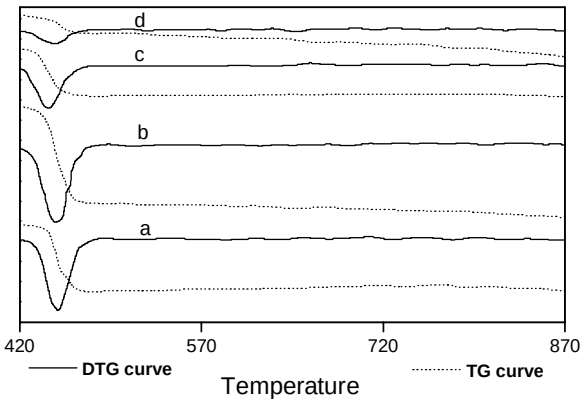

Fig. 2. TG (dash lines) and DTG (solid lines) curves during TPR of: CM1 (a); CM2 (b); CM3 (c) and CM4 (d).

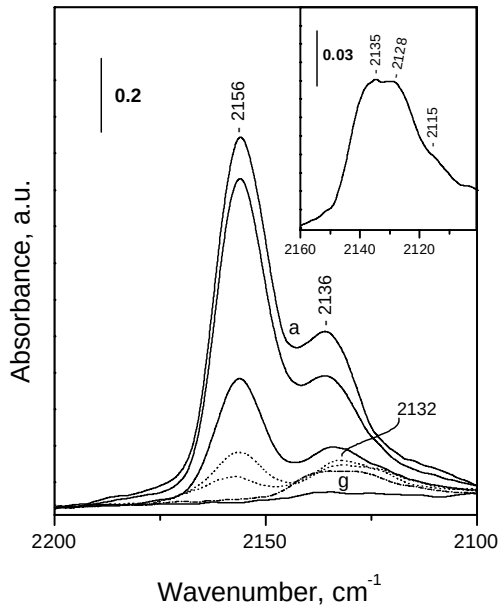

Fig. 3. FTIR spectra of CO (1.3 kPa equilibrium pressure) adsorbed at 85 K on CM1 (a); after evacuation at 100 K (b–e); during a gradual increase of temperature (f) and at 373 K (g). All spectra are background corrected.

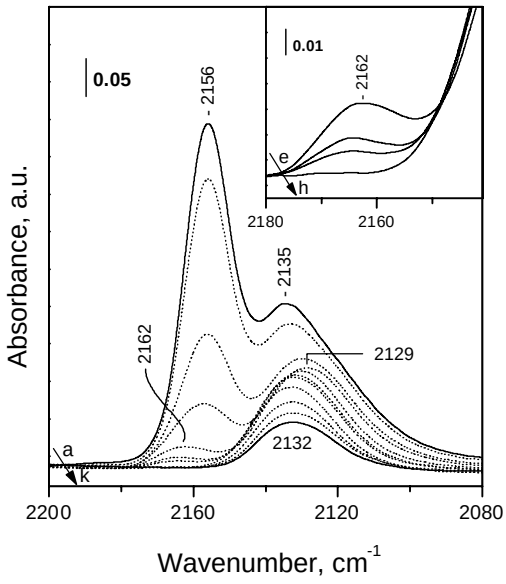

Fig. 4. FTIR spectra of CO (700 Pa equilibrium pressure) adsorbed at 85 K on CM2 (a) and after evacuation at 100 K (b–g) and during a gradual increase of temperature (h–k). All spectra are background corrected.

spectra c–e). This band consists of at least three components (around 2135, 2128 and 2115 cm^{-1}). The band is resistant towards evacuation at ambient temperature (Fig. 3, spectrum f) and disappears completely after evacuation at 373 K (Fig. 3, spectrum g). The band position and stability indicate that it is due to Cu^{+}–CO species [66–71]. The relatively high stability of these entities originates from the synergism between σ and π-components of the Cu^{+}–CO bond. It should be noted that Cu^{0}–CO species could also be observed around 2130 cm^{-1} but they are, as a rule decomposed even at low temperature [72]. The results indicate some heterogeneity of the Cu^{+} cations in the sample.

3.2.2. CO adsorption on reduced CM1

The sample was reduced in 13.3 kPa H_2 and then evacuated at 523 K. Adsorption of CO (400 Pa equilibrium pressure) on the sample thus treated, led again to the appearance of two intense bands, at 2156 and 2136 cm^{-1}, which had already been attributed to H-bonded and physically adsorbed CO, respectively (spectra not shown). Decrease in the equilibrium pressure caused vanishing of these two bands, thus revealing a broad weak component centered at 2127 cm^{-1}. However, in contrast to the case of the oxidized sample, the band at 2127 cm^{-1} was easily removed during evacuation even at temperatures lower than the ambient one. This allows assignment of the 2127 cm^{-1} band to Cu^{0}–CO carbonyls, which is consistent with the TPR results indicating an almost complete reduction of copper under the conditions applied. Generally the carbonyls of metallic copper absorb at lower frequencies than the Cu^{+}–CO species (as observed here) but there are many exceptions to this rule [57]. Here again, a heterogeneity of the copper sites has been found.

3.2.3. CO adsorption on oxidized CM2

In this case again low-temperature CO adsorption results in the appearance of two intense bands: H-bonded CO at 2156 cm^{-1} and physically adsorbed CO at 2135 cm^{-1} (Fig. 4, spectrum a). Careful analysis of the spectrum shows however that here, the band at 2134 cm^{-1} has a low-frequency shoulder. Coverage decrease allows a more precise location of this shoulder, its maximum being at 2129 cm^{-1} (Fig. 4, spectrum c). The 2156 cm^{-1} band disappears and a weak band at 2162 cm^{-1} becomes clearly visible (Fig. 4, spectrum e). The lower frequency band is converted to a well-shaped band at 2129 cm^{-1}.

Additional decrease in coverage leads to an intensity drop of the 2162 and 2129 cm^{-1} bands and to a development of a new, coverage independent band at 2132 cm^{-1} (Fig. 4, spectra e–k). The latter is highly resistant to evacuation and disappears from the spectrum after evacuation at 373 K (spectra not shown).

The above results can be rationalized assuming formation of $Cu^{+}(CO)_2$ species (ν_{as} at 2162 and ν_s at 2129 cm^{-1}) which are converted to Cu^{+}–CO monocarbonyls (2132 cm^{-1}). There are many works reporting formation of copper di- (and even tri-) carbonyls after CO adsorption on zeolites [58–63]. However, typically the ν_{as} and ν_s modes are observed around 2178 and 2151 cm^{-1}. The formation of polycarbonylic species has been explained by the low coordination of the cations in zeolites and is not typical of the Cu^{+}–CO system [60]. Thus, many studies of CO adsorption on oxide-supported copper report exclusively formation of monocarbonyls. Zecchina and co-workers [65] were the first to report formation of dicarbonyls after low-temperature CO adsorption on Cu-SiO_2 and Cu_2O (frequencies at 2162–2150 and 2132–2113 cm^{-1}). We have

also recently reported similar species formed on Cu/SiO_2 [64], Cu/TiO_2 [66] and Cu/MCM-41 [67] samples.

3.2.4. CO adsorption on reduced CM2

The sample was reduced at two temperatures, namely 523 and 673 K, in 16 kPa H_2, each reduction followed by evacuation at the same temperature.

Low-temperature CO adsorption (530 Pa equilibrium pressure) on the 523 K reduced sample leads to the appearance of two main bands at 2156 cm^{-1} (H-bonded CO) and 2123 cm^{-1}. In addition, a weak band at 2182 cm^{-1} is clearly observable (spectra not shown). Evacuation leads to decrease in intensity and disappearance of the bands at 2182 and 2156 cm^{-1}. Difference spectra indicate that the band at 2123 cm^{-1} loses quickly two components, around 2137 cm^{-1} (physically adsorbed CO) and 2112 cm^{-1}, a small decrease of a component at ca 2125 cm^{-1} being also observed. The band at 2112 cm^{-1} can be attributed to Cu^0–CO species indicating the existence of reduced copper sites. When the band at 2156 cm^{-1} disappears, a component at 2161 cm^{-1} is visible. The low-frequency band is slightly blue shifted initially to 2127 and then to 2129 cm^{-1}. The latter decreases in intensity but does not disappear even after evacuation at ambient temperature.

The bands at 2161 and ca. 2127 cm^{-1} are attributed, by analogy with the oxidized sample, to the ν_s and ν_{as}, respectively, of $Cu^+(CO)_2$ species. The band at 2129 characterizes the corresponding monocarbonyls.

According to its position, the band at 2182 cm^{-1} in the spectrum could be assigned to Cu^{2+}–CO species. However, it is not likely to have Cu^{2+} ions on the reduced sample. That is why we assign this band to $Cu^+(CO)_2$ dicarbonyls. In fact, the band position is very similar to the ν_s modes observed with copper dicarbonyls on Cu-ZSM-5 [58–61] and even on Cu/silicalite-1 [62]. Evidently, the respective ν_{as} modes (expected around 2151 cm^{-1}) are masked by the strong OH–CO band at 2156 cm^{-1}. Thus, the results suggest that this reduction treatment has led to creation of Cu^+ cations that are similar to cations in zeolites. The corresponding Cu^{2+} ions are relatively stable and not reduced to Cu^+ under vacuum.

The spectra registered after CO adsorption (270 Pa equilibrium pressure) on the sample reduced at 673 K are presented in Fig. 5. The main differences observed with the sample reduced at 523 K are as given further.

- The band at 2182 cm^{-1} is absent, which means that the respective Cu^+ sites have been reduced.
- The band at 2161 cm^{-1} and its lower frequency counterpart have a negligible intensity demonstrating that the main fraction of the corresponding Cu^+ sites has also been reduced.
- The band at 2129 cm^{-1} almost disappears after evacuation at temperatures lower than the ambient one, which indicates that the copper is mainly in the Cu^0 state.

The overall intensity of the bands around 2130 cm^{-1} is reduced. Although we have no data about the extinction coefficient of the different copper carbonyls, the results are consistent with the formation of copper particles where some of the copper atoms are in the bulk and thus not accessible to CO.

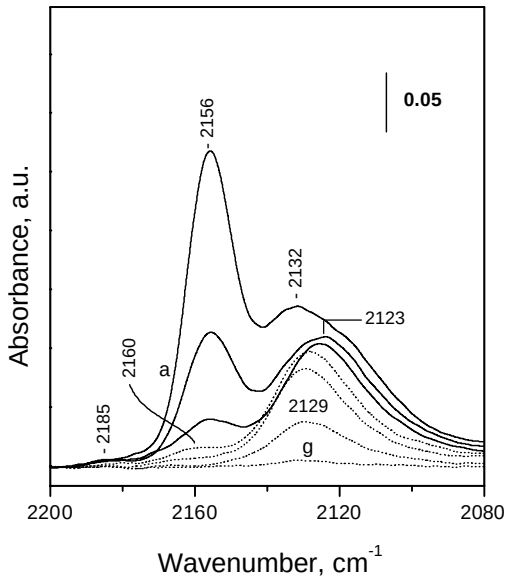

Fig. 5. FTIR spectra of CO (270 Pa equilibrium pressure) adsorbed at 100 K on CM2 reduced at 673 K (a); after evacuation at 100 K (b–d) and during a gradual increase of temperature (e–g). All spectra are background corrected.

3.2.5. CO adsorption on oxidized CM3

Adsorption of CO (266 Pa equilibrium pressure) at 100 K on the vacuum activated sample results in the appearance of several IR bands in the spectrum. Their maxima are at 2198, 2185 (sh), 2156 (s), 2132 and 2123 cm^{-1} (Fig. 6, spectrum

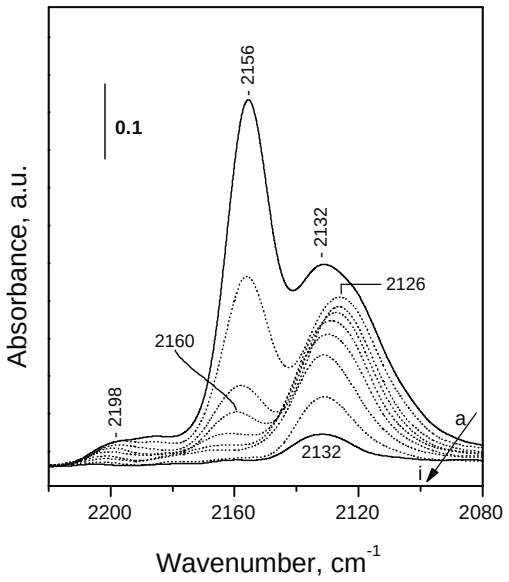

Fig. 6. FTIR spectra of CO (270 Pa equilibrium pressure) adsorbed at 85 K on CM3 (a) and after evacuation at 100 K (b–e) and during a gradual increase of temperature (f–i). All spectra are background corrected.

a). The 2156 cm^{-1} band is due to H-bonded CO and declines with evacuation (Fig. 6, spectra b–d). As in the previous cases, a band at 2161 cm^{-1}, more resistant to evacuation, is well discernible at lower coverages (Fig. 6, spectrum d). The band at 2132 cm^{-1} (physically adsorbed CO) vanishes very quickly leaving, in the spectrum, an asymmetric band at 2126 cm^{-1}. The weak band at 2185 cm^{-1} also strongly decreases in intensity during evacuation, while the band at 2198 cm^{-1} remains almost unaffected. Additional evacuation (Fig. 6, spectra e–i) results in:

- decrease in intensity/disappearance of the band at 2161 cm^{-1} and simultaneous shift of the band at 2127 cm^{-1} to 2132 cm^{-1}. Then the latter band decreases in intensity without changing its position;
- decrease in intensity/disappearance of the band at 2198 cm^{-1} with a simultaneous blue shift to ca. 2202 cm^{-1}.

Taking into account the results with the other samples, we propose the following assignment. The set of bands at 2161 and 2127 cm^{-1} characterize dicarbonyls of Cu^{+} ions whereas the corresponding monospecies absorb at 2132 cm^{-1}; the band at 2185 cm^{-1} arises from another kind of dicarbonyl species formed with Cu^{+} in positions similar to cationic positions in zeolites; the band at 2198 cm^{-1} (not observed with the CM1 and CM2 samples) is assigned, in agreement with literature data [77], to Cu^{2+}–CO species. The principal band registered after room temperature evacuation, is that of Cu^{+}–CO species at 2132 cm^{-1}. A weak band around 2160 cm^{-1} is also noticed and most probably it corresponds to monocarbonyls with Cu^{+} ions in cationic positions.

Thus, the main difference between this sample and the CM1 and CM2 specimens appears to be the existence of accessible Cu^{2+} cations in the former case.

3.2.6. CO adsorption on reduced CM3

Introduction of 266 Pa CO to the reduced sample at 100 K results in the appearance of two intense bands in the IR spectrum, their maxima being at 2155 and 2118 cm^{-1} (Fig. 7, spectrum a). Decrease of the coverage during evacuation initially does not affect the 2118 cm^{-1} band but the band at 2155 cm^{-1} decreases (Fig. 7, spectrum b) Additional coverage decrease is accompanied by a further intensity drop of the 2155 cm^{-1} band and its disappearance (Fig. 7, spectra c–e). A weak component at 2159 cm^{-1} is then revealed. The 2118 cm^{-1} band first slightly rises in intensity and is shifted to 2120 cm^{-1} then starts to decline and its maximum is settled at 2124 cm^{-1} (Fig. 7, spectra f, g). The band quickly disappears from the spectrum after evacuation at temperatures above 100 K (Fig. 7, spectra h–l). The low stability of the band implies that it characterizes Cu^{0}–CO species. Here the band at 2159 cm^{-1} as well as the behavior of the lower frequency band resemble the spectra obtained after CO adsorption on Cu^{+} cations. The origin of this phenomenon is far from clear. We could suggest formation of dicarbonyls on metallic copper sites.

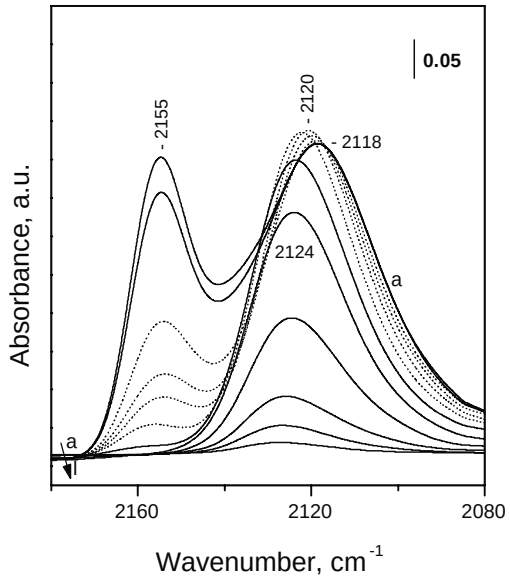

Fig. 7. FTIR spectra of CO (270 Pa equilibrium pressure) adsorbed at 100 K on CM3 reduced at 673 K (a); after evacuation at 100 K (b–g) and during a gradual increase of temperature (h–l). All spectra are background corrected.

3.2.7. CO adsorption on oxidized CM4

The spectra (Fig. 8) obtained after adsorption of CO at low temperature on the vacuum activated CM4 sample are essentially the same as those registered with the CM3 sample (see Fig. 6). This suggests that the copper state on both samples is almost identical.

3.2.8. CO adsorption on reduced CM4

Here again, the spectra (not shown) are similar to those obtained with the reduced CM3 sample (see Fig. 7). The main

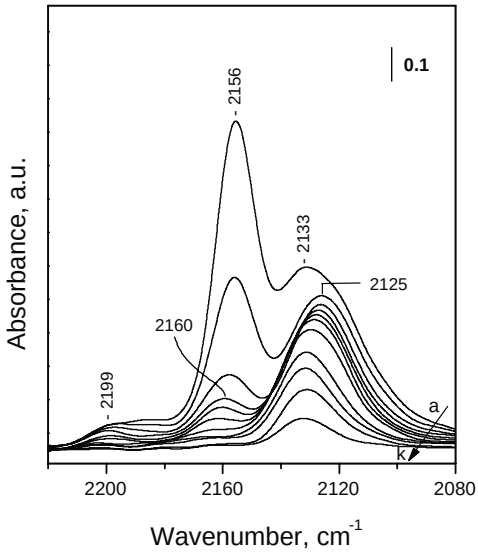

Fig. 8. FTIR spectra of CO (270 Pa equilibrium pressure) adsorbed at 100 K on CM4 (a) and after evacuation at 100 K (b–f) and during a gradual increase of temperature (g–k). All spectra are background corrected.

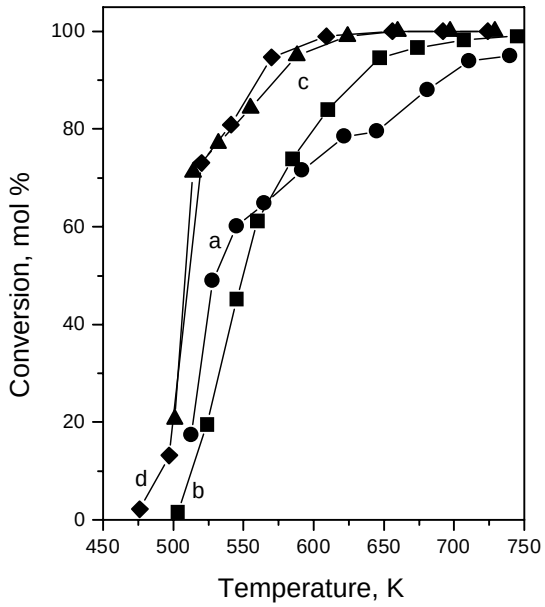

Fig. 9. Methanol conversion vs. temperature on the oxidized samples: CM1 (a); CM2 (b); CM3 (c) and CM4 (d).

difference is that with CM4 the frequencies of the Cu^0–CO species are somewhat lower: 2113 cm^{-1} at saturation and 2119 cm^{-1} at intermediate and low coverages. In the latter cases the band is clearly seen to consist of two components, namely at 2124 and 2119 cm^{-1}. The results are indicative of some heterogeneity of the copper in this sample. Generally, the higher frequencies of CO adsorbed on metallic copper are suggesting a higher surface roughness. Usually this is associated with a higher copper dispersion, but such conclusions are not unambiguous.

3.3. Catalytic test

The plots of methanol conversion versus temperature on the oxidized samples are presented in Fig. 9. The values of

Table 2
MF selectivity on the investigated samples at comparable conversion

Samples	MF selectivity (mol.%)			
	CM1	CM2	CM3	CM4
Oxidized	53	52	38	20
Reduced	75	60	50	62

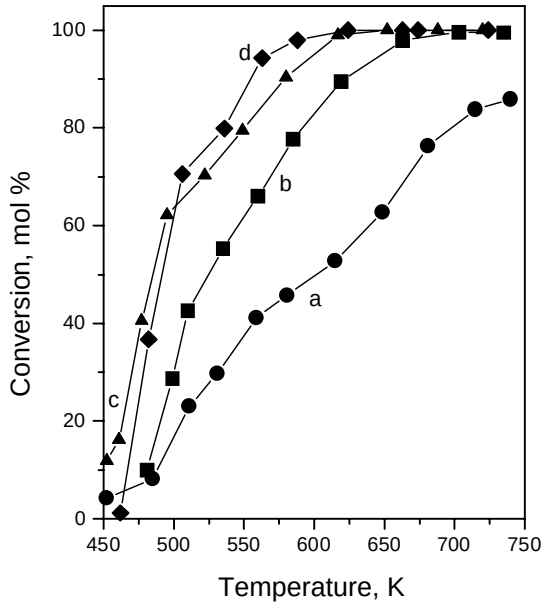

Fig. 11. Methanol conversion vs. temperature on the reduced samples: CM1 (a); CM2 (b); CM3 (c) and CM4 (d).

MF selectivity for the samples are also given in Table 2. They were estimated at a conversion degree of about 50 and 40% for the oxidized and reduced samples, respectively. All catalysts exhibit activity above 500 K and a higher conversion is registered for CM3 and CM4. The distribution of MF and CO is essentially different for all studied samples. The MF selectivity (see Table 2) is higher for CM1 and

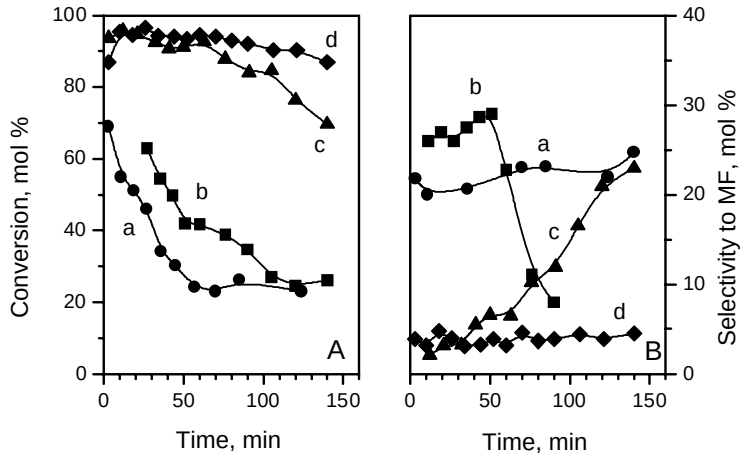

Fig. 10. Methanol conversion (A) and MF selectivity (B) vs. the time on stream on the oxidized samples: CM1 (a); CM2 (b); CM3 (c) and CM4 (d).

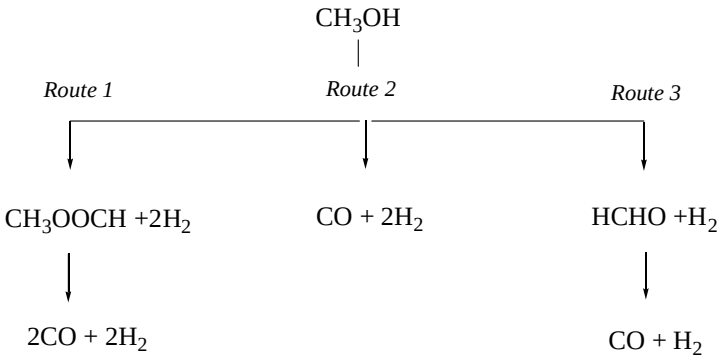

Scheme 1.

CM2 and significantly decreases with CM3 and especially with CM4.

The catalysts preserve their arrangement in the methanol conversion under isothermal conditions at 600 K (Fig. 10). However, in contrast to CM3 and CM4, a rapid decrease in methanol conversion for CM1 and CM2 is observed (Fig. 10A). A specific dependence of the selectivity changes with the time on stream for each sample is found (Fig. 10B). MF selectivity rapidly decreases for CM2 and increases for CM3, while it remains almost unchanged for about 2 h with CM1 and CM4.

All reduced samples exhibit a higher catalytic activity and selectivity towards MF as compared to the corresponding oxidized materials (Fig. 11 and Table 2).

4. Discussion

The control of methanol dehydrogenation selectivity is complicated due to the fact that proceeding of different reactions is possible (Scheme 1) [14,15,30]. They differ essentially in their thermodynamics [30,78] and could be favored to different extents depending on the catalyst peculiarities [17,19,21–24,27–30,34,44]. The catalyst preparation method is a promising way of regulating different reaction pathways but more information on the nature of the active sites and their specific catalytic behavior is needed. In the case of copper-containing catalysts the literature data concerning the role of various copper species in this process are rather controversial. Usually the participation of metallic copper is reported [11–13,16,18–20,23–26,32,33,42,45,46] but the role of copper ions in this process is not completely clear [12,14,17,21,22,28,29,31,43,44,47,48]. In our previous studies [79–84], the nature of a catalytic active complex (CAC) of copper modified activated carbon in methanol decomposition has been discussed. The participation of CAC, comprising copper species in different oxidative states, bonded both with functional groups of the support and between themselves, is proposed. In the following section we discuss the effect of copper species (created by different preparation methods) on the various methanol dehydrogenation pathways (Scheme 1).

4.1. State of copper on the samples

On the basis of the combined physicochemical and catalytic studies two representative series of the investigated samples could be distinguished. The samples from Series I (CM1 and CM2) contain predominantly CuO entities and practically no Cu^{2+} ions are observed with the activated samples (Figs. 3 and 4). However, a somewhat higher dispersion (Fig. 1) and a lower reducibility (Table 1) are found for the CM2 sample as compared to CM1. Both samples exhibit similar catalytic activities (Fig. 9), a low stability (Fig. 10A) and relatively high MF selectivity in methanol decomposition (Table 2).

The samples from Series II (CM3 and CM4), are characterized by the presence of both highly dispersed CuO species and Cu^{2+} ions strongly interacting with the support (Figs. 6 and 8). The relative part of the latter is greater in the case of CM4. Only partial reduction of the copper species even at 870 K is established for both samples (Fig. 2, Table 1). CM3 and CM4 are characterized by a higher catalytic activity (Fig. 9), a higher stability (Fig. 10A) and a significantly lower selectivity to MF (Table 2) as compared to the samples from Series I.

A well defined tendency to an increase in catalysts activity (Fig. 11) and MF selectivity (Table 2) is registered with all samples after their reduction in hydrogen. The predominant formation of Cu^0 is observed by FTIR spectroscopy and by XRD (not shown). It should be noted that the presence of copper ions in the oxidized CM3 and CM4 is a factor favoring the higher dispersion of the metallic copper after their reduction (see Sections 3.2.6 and 3.2.8).

4.2. Mechanism of methanol decomposition

As was mentioned above (see Section 4.1), both samples from each series are characterized by similar catalytic activity (Fig. 9) and MF selectivity (Table 2) in methanol dehydrogenation. However, some essential differences in their catalytic behaviour under isothermal conditions (Fig. 10) or after their hydrogen pretreatment (Fig. 11) are observed. In the latter case, an increase in the catalytic activity and MF selectivity is established for all samples (Fig. 11, Table 2).

Obviously these peculiarities could not be explained by the differences in copper dispersion (estimated on the basis of the TPR experiments, XRD and FTIR spectra) only. Taking into account the results from the FTIR experiments (see Section 4.1), we assume that various copper species take part in the methanol dehydrogenation. It could be concluded that predominantly Cu^0 participate in the formation of MF while the methanol dehydrogenation to CO is favoured by the presence of copper ions in the samples. This conclusion is also in accordance with the results of other authors [29], where the high CO selectivity in methanol decomposition is assigned to copper ions in CuZSM-5.

On the basis of the results obtained two general effects should be mentioned: (i) an increase in the catalytic activity in the presence of copper ions (oxidized CM3 and CM4) or metallic copper (all reduced samples); (ii) an increase in CO or MF selectivity for the samples containing predominantly copper ions or metallic copper, respectively. Hence, different pathways of methanol decomposition (Scheme 1) on various copper species could be proposed. The mechanism of CO formation from MF (as an intermediate product) is possible in the presence of Cu^0 species (Scheme 1, route 1). On the contrary, the higher selectivity towards CO, combined with the higher catalytic activity found for the samples from Series II, suggest the formation of CO directly from methanol in presence of cationic copper entities (Scheme 1, route 2). The kinetic curves (Fig. 10) give additional evidence in this aspect. Here, the MF selectivity gradually increases with time on stream for CM3 or remains almost unchanged for CM4. In accordance with the TPR data (Table 1), the more significant changes in the copper oxidative state for CM3 due to the reductive reaction medium could be the reason for the results observed.

The kinetic data on CM1 and CM2 selectivity are more complicated (Fig. 10B). In spite of the similarity in activity changes of the two samples (Fig. 10A), a considerable difference in the shape of their selectivity curves is found (Fig. 10B). A significant decrease in the MF selectivity is only observed in the case of CM2, while it is preserved almost unchanged for CM1. At the same time, for both samples only CuO species are registered, although some differences in their dispersion are also found (see Section 4.1). The dependence of the catalytic selectivity on the copper particle size suggests the participation in methanol dehydrogenation to MF of catalytic sites with a complex structure [79–84], containing two or more neighboring copper species.

5. Conclusion

Depending on the preparation method used, samples with different ratio between CuO species and isolated copper ions could be obtained. The Cu^{2+} ions strongly interacting with MCM-41 surface are highly resistant to reduction. Their presence favours a high copper dispersion in the reduced catalysts. The participation of different copper species in the various methanol dehydrogenation pathways is assumed. The regulation of their ratio by the preparation method used could be a possible way for the methanol dehydrogenation selectivity control.

Acknowledgements

Financial support from the Bulgarian National Research Foundation (Projects X-1205) and Bulgarian Academy of Sciences is gratefully acknowledged. K. Hadjiivanov is indebted to the Alexander von Humboldt-Foundation. C. Minchev also thanks the Deutscher Akademischer Austauschdienst for the donation of a Bruker Vector 22 FTIR spectrometer and to Dr. R. Köhn (Hamburg) and Prof. M. Fröba (Giessen) for the support and helpful discussions.

References

[1] J.S. Lee, J.C. Kim, Y.G. Kim, Appl. Catal. 57 (1990) 1.
[2] I. Winder, Catal. Rev.-Sci. Eng. 26 (1985) 3.
[3] W.H. Calkins, Catal. Rev.-Sci. Eng. 26 (1985) 47.
[4] M. Roeper, Erdoel Kohle Erdgas Petrochem. 37 (1987) 506.
[5] W.H. Cheng, H.H. Kung, in: W.H. Cheng, H.H. Kung (Eds.), Methanol Production and Use, New York: Marcel Dekker, 1994 (Chapter 1).
[6] A. Yildiz, K. Pekmez, in: Y. Yürüm (Ed.), Hydrogen Energy System, NATO ASI Series., Ser. E Appl. Sci., vol. 295, Kluwer Academic Publishers, Netherlands, 1995, p. 195.
[7] L. Pettersson, K. Sjoestroem, Combust. Sci. Technol. 80 (1991) 265.
[8] Decomposed Methanol Workshop Report, Alternative Fuels Utilisation Contractors, Co-ordination Meeting, US Department of Energy, Windsor, Ont., 1983.
[9] W.H. Cheng, Acc. Chem. Res. 32 (1999) 685.
[10] J. Zawadzki, B. Azambre, O. Heintz, A. Krzton, J. Weber, Carbon 38 (2000) 509.
[11] W.H. Cheng, Mater. Chem. Phys. 41 (1995) 36.
[12] W.H. Cheng, Appl. Catal. A 130 (1995) 13.
[13] W.H. Cheng, C.Y. Shiau, T.H. Liu, H.L. Tung, J.F. Lu, C.C. Hsu, Appl. Catal. 170 (1998) 215.
[14] I. Shlegel, D. Gutshik, A.Ya. Rozovskii, Kinet. Katal. 31 (1990) 1000 (in Russian).
[15] S.V. Gorshkov, G.J. Lin, A.Ya. Rozovskii, Kinet. Katal. 40 (1999) 334 (in Russian).
[16] W.H. Cheng, C.Y. Shiau, T.H. Liu, H.L. Tung, J.F. Lu, C.C. Hsu, Appl. Catal. B 13 (1998) 63.
[17] N.W. Cant, S.P. Tonner, D.L. Trimm, M.S. Wainwright, J. Catal. 91 (1985) 197.
[18] W.H. Cheng, Appl. Catal. B 7 (1995) 127.
[19] T. Sodesawa, M. Nagacho, A. Onodera, F. Nozaki, J. Catal. 102 (1986) 460.
[20] S. Sato, M. Iijima, T. Nakayama, T. Sodesawa, F. Nozaki, J. Catal. 169 (1997) 47.
[21] K. Hashimoto, N. Toukai, J. Mol. Catal. A 186 (2002) 79.
[22] M. Clement, Y. Zhang, D.S. Brands, E.K. Poels, A. Bliek, Stud. Surf. Sci. Catal. 130 (2000) 2123.
[23] G.P. Salomatin, V.S. Sobolevskii, V.V. Grigoriev, L.I. Lafer, V.I. Jackerson, Izv. AN SSSR, Ser. Khim. 10 (1981) 2204 (in Russian).
[24] I.A. Fisher, A.T. Bell, J. Catal. 184 (1999) 357.
[25] D.B. Clarke, D.K. Lee, M.J. Sandoval, A.T. Bell, J. Catal. 150 (1994) 81.
[26] L. Domokos, T. Katona, A. Molnar, Catal. Lett. 40 (1996) 215.

[27] M. Ai, Appl. Catal. 11 (1984) 259.
[28] K. Takagi, Y. Moricawa, T. Ikawa, Chem. Lett. (1985) 527.
[29] Z.T. Liu, D. Shun, Z.Y. Guo, Appl. Catal. A 118 (1994) 163.
[30] T.P. Minyukova, I.I. Simentsova, A.V. Khasin, N.V. Shtertser, N.A. Baronskaya, A.A. Khassn, T.M. Yurieva, Appl. Catal. A 237 (2002) 171.
[31] A. Iimura, Y. Inoue, I. Yasumori, Bull. Chem. Soc. Jpn. 56 (1983) 2203.
[32] S.P. Tonner, M.S. Wainwright, D.L. Trimm, N.W. Cant, Appl. Catal. 1 (1984) 93.
[33] A.L. Lapidus, S.N. Antonyuk, V.D. Kapkin, L.A. Bruk, S.D. Sominskii, N.S. Nechuro, Neftechim 25 (1985) 761 (in Russian).
[34] E.H. Shreiber, M.D. Rhodes, G.W. Roberts, Appl. Catal. B 23 (1999) 9.
[35] E.H. Shreiber, G.W. Roberts, Appl. Catal. B 26 (2000) 119.
[36] G.J. Milar, C.H. Rochester, K.C. Waugh, J. Chem. Soc., Faraday Trans. 87 (1991) 2795.
[37] I.E. Wachs, R.J. Madix, J. Catal. 53 (1978) 208.
[38] B.A. Sexton, A.E. Hughes, N.R. Avery, Appl. Surf. Sci. 22/23 (1985) 404.
[39] C. Barnes, T. Pudney, Q. Guo, M. Bowker, J. Chem. Soc., Faraday Trans. 86 (1990) 2693.
[40] S.S. Fu, G.A. Somorjai, J. Phys. Chem. 96 (1992) 4542.
[41] R. Ryberg, J. Chem Phys. 82 (1985) 567.
[42] A. Guerro-Ruiz, I. Rodriguez Ramos, J.L.G. Fierro, Appl. Catal. 72 (1991) 119.
[43] S. Poulston, E. Rowbotham, P. Stone, M. Bowker, Catal. Lett. 52 (1998) 63.
[44] A. Music, J. Batista, J. Levec, Appl. Catal. A 165 (1997) 115.
[45] T. Matsuda, K. Yogo, Ch. Pantawong, E. Kikuchi, Appl. Catal. A 142 (1996) 151.
[46] Y. Wang, R. Gang, S. Han, React. Kinet. Catal. Lett. 67 (1999) 305.
[47] Y. Morikawa, Adv. Catal. 39 (1993) 303.
[48] E.D. Guerreiro, O.F. Gorriz, J.B. Rivarola, L.A. Arrua, Appl. Catal. A 165 (1997) 259.
[49] H. Imai, K. Nakamura, J. Catal. 125 (1990) 571.
[50] A. Corma, Chem. Rev. 97 (1997) 2373.
[51] F. Schüth, A. Wingen, J. Sauer, Microporous Mesoporous Mater. 44–45 (2001) 465.
[52] U. Ciesla, F. Schüth, Microporous Mesoporous Mater. 27 (1999) 131.
[53] R. Köhn, M. Fröba, Catal. Today 68 (2001) 227.
[54] M. Hartmann, Stud. Surf. Sci. Catal. 128 (2000) 215.
[55] M. Ziolek, I. Sobczak, P. Decyk, I. Nowak, Stud. Surf. Sci. Catal. 125 (1999) 633.
[56] A. Zecchina, D. Scarano, G. Spoto, S. Bordiga, C. Lamberti, G. Bellussi, Stud. Surf. Sci. Catal. 117 (1998) 343.
[57] K.I. Hadjiivaniov, G.N. Vayssilov, Adv. Catal. 47 (2002) 307.
[58] G. Spoto, A. Zecchina, S. Bordiga, G. Ricchiardi, C. Martra, G. Leofanti, G. Petrini, Appl. Catal. B 3 (1994) 151.
[59] T. Pieplu, F. Poignant, A. Vallet, J. Saussey, J.-C. Lavalley, Stud. Surf. Sci. Catal. 96 (1995) 619.
[60] K. Hadjiivanov, M. Kantcheva, D. Klissurski, J. Chem. Soc., Faraday Trans. 92 (1996) 4595.
[61] K. Hadjiivanov, H. Knözinger, J. Catal. 191 (2000) 480.
[62] A. Milushev, K. Hadjiivanov, Phys. Chem. Chem. Phys. 3 (2001) 5337.
[63] H. Miessner, H. Landmesser, N. Jaeger, K. Richter, J. Chem. Soc., Faraday Trans. 93 (1997) 3417.
[64] K. Hadjiivanov, H. Knözinger, Phys. Chem. Chem. Phys. 3 (2001) 1132.
[65] D. Scarano, S. Bordiga, C. Lamberti, G. Spoto, G. Richiardi, A. Zecchina, C. Otero Arean, Surf. Sci. 411 (1998) 272.
[66] T. Venkov, K. Hadjiivanov, Catal. Commun. 4 (2003) 209.
[67] K. Hadjiivanov, T. Tsoncheva, M. Dimitrov, C. Minchev, H. Knözinger, Appl. Catal. A 241 (2003) 331.
[68] J.M.G. Amores, V. Sanchez Escribano, G. Busca, V. Lorenzelli, J. Mater. Chem. 41 (1994) 965.
[69] K. Hadjiivanov, M. Kantcheva, D. Klissurski, J. Chem. Soc., Faraday Trans. 92 (1996) 4595.
[70] A. Dandekar, M.A. Vannice, Appl. Catal. B 22 (1999) 179.
[71] B. Padley, C.H. Rochester, G.H. Hutchings, F. Kung, J. Catal. 148 (1994) 438.
[72] P. Hollins, Surf. Sci. Rep. 16 (1992) 51.
[73] A.R. Balkenende, C.J.G. van der Grift, E.A. Meulenkamp, J.W. Geus, Appl. Surf. Sci. 68 (1993) 161.
[74] C. Minchev, R. Köhn, T. Tsoncheva, M. Dimitrov, I. Mitov, D. Paneva, H. Huwe, M. Fröba, Stud. Surf. Sci. Catal. 142 (2002) 1245.
[75] C. Minchev, R. Köhn, T. Tsoncheva, M. Dimitrov, M. Fröba, Stud. Surf. Sci. Catal. 135 (2001) 235.
[76] K. Hadjiivanov, D. Klissurski, M. Kantcheva, A. Davydov, J. Chem. Soc., Faraday Trans. 87 (1991) 907.
[77] K. Hadjiivanov, H. Knözinger, J. Catal. 191 (2000) 480.
[78] D.R. Stull, E.F. Westrum, G.C. Sinke, The Chemical Thermodynamics of Organic Compounds, Wiley, New York, 1969, p. 450.
[79] T. Tsoncheva, Compt. Rend. Acad. Bulg. Sci. 54 (2001) 65.
[80] T. Tsoncheva, Compt. Rend. Acad. Bulg. Sci. 54 (2001) 59.
[81] R. Nickolov, T. Tsoncheva, D. Mehandjiev, Fuel 81 (2001) 203.
[82] T. Tsoncheva, S. Vankova, D. Mehandjiev, Fuel 82 (2003) 755.
[83] T. Tsoncheva, R. Nickolov, Y. Neinska, Chr. Minchev, D. Mehandjiev, Bulg. Chem. Commun. 32 (2000) 218.
[84] T. Tsoncheva, R. Nickolov, D. Mehandjiev, React. Kinet. Catal. Lett. 72 (2001) 383.